Fast-electron-impact study on excitations of 4d electron of xenon*

Zhang Xin(张 鑫)[a)b)], Liu Ya-Wei(刘亚伟)[a)b)], Peng Yi-Geng(彭裔耕)[a)b)],
Xu Long-Quan(徐龙泉)[a)b)], Ni Dong-Dong(倪冬冬)[a)b)], Kang Xu(康 旭)[a)b)],
Wang Yang-Yang(王洋洋)[a)b)], Qi Yue-Ying(祁月盈)[c)], and Zhu Lin-Fan(朱林繁)[a)b)†]

[a)] *Hefei National Laboratory for Physical Sciences at Microscale and Department of Modern Physics, University of Science and Technology of China, Hefei* 230026, *China*
[b)] *Synergetic Innovation Center of Quantum Information and Quantum Physics, University of Science and Technology of China, Hefei* 230026, *China*
[c)] *School of Mathematics, Physics, and Information Engineering, Jiaxing University, Jiaxing* 314001, *China*

(Received 26 June 2015; revised manuscript received 26 August 2015; published online 20 October 2015)

The electron energy loss spectrum of the 4d excitations of xenon was measured at an incident electron energy of 1500 eV and a scattering angle of 6°. Besides the optically allowed transitions of $4d_{5/2}^{-1}np$ and $4d_{3/2}^{-1}np'$, the optically forbidden transitions of $4d_{5/2}^{-1}ns$, $4d_{5/2}^{-1}nd$, $4d_{3/2}^{-1}ns'$, and $4d_{3/2}^{-1}nd'$ were observed. The measured features are assigned with the help of the calculation by the Cowan Code. The line profile parameters of both optically allowed transitions and optically forbidden ones were determined and compared with the previous available data. It is found that the natural widths of both dipole-allowed and dipole-forbidden excitations are approximately identical, which means the spectator transitions dominate the resonant Auger effect for both dipole-allowed and dipole-forbidden transitions.

Keywords: electron energy loss spectrum, optically forbidden transition, natural width

PACS: 34.80.Dp, 32.80.Aa, 32.80.Hd **DOI:** 10.1088/1674-1056/24/12/123401

1. Introduction

The energy level structures of atoms and molecules are of great importance from the viewpoints of both the fundamental researches and the applications. The inner-shell excitations of atoms and molecules have been paid special attention since the investigations about them reveal abundant physical information such as the electron correlation and exchange effects, the interference effect between the direct ionization, autoionization and fluorescence de-excitation processes, as well as the decay mechanism of the participator or spectator Auger process.[1–5] Furthermore, the inner-shell excitations of atoms and molecules, especially those of the noble gases and nitrogen, have been used to test and calibrate the monochromator used in synchrotron radiation.[6–8] Although nowadays the energy level structures of the valence-shell excitations of atoms and molecules have been well studied and summarized, the knowledge of their inner-shell excitations is relatively scarce. The reason may be due to the fact that the high excitation energy of the inner-shell state is difficult to achieve by the traditional light source and laser. The early investigations about the inner-shell excitations of atoms and molecules were carried out by the high-energy electron energy loss spectroscopy (EELS)[9–11] and the synchrotron radiation,[12–18] and recently most works were made by the synchrotron radiation with its dramatic progress.[19–22] However, only the dipole-allowed transitions are achieved by the synchrotron radiation and the EELS operated at the optical limit, i.e., the momentum transfer is near zero at a scattering angle of 0° which is the most used condition in previous investigations.[9,10] So the abundant dipole-forbidden inner-shell excitations have seldom been explored experimentally,[23–27] and this is the main purpose of this work.

As for xenon, its inner-shell excitations were investigated by the synchrotron radiation[12–14,18–21] and high-energy EELS[9,28] experimentally. More specifically, the experimental energy level positions and the natural widths for the dipole-allowed 4d excitations have been reported by Refs. [9], [18], [19], and [21]. Although the energy positions of the 4d excitations reported by different groups[9,18] are in good agreement, the experimental natural widths show large discrepancies. The natural widths of the $4d^{-1}np$ excitations determined by King *et al.*[9] show a slight tendency of increase with the principal quantum number n, while the results of Masui *et al.*[21] are nearly constant and their results are generally lower than others. However, the more recent work of Sairanen *et al.*[19] gives a slight tendency of decrease in natural widths with the higher n for the resonances in both series of $4d_{5/2}^{-1}np$ and $4d_{3/2}^{-1}np'$. It should be pointed out that all works just mentioned were mea-

*Project supported by the National Natural Science Foundation of China (Grant Nos. U1332204, 11274291, 11504361, and 11320101003).
†Corresponding author. E-mail: lfzhu@ustc.edu.cn
© 2015 Chinese Physical Society and IOP Publishing Ltd

sured with the synchrotron radiation and high-energy EELS operated at a scattering angle of 0°, and the features of the dipole-allowed transitions dominate. Considering that there is a small momentum transfer at the scattering angle of 0° by the high-energy EELS due to the finite angular resolution, the optically forbidden transitions of $4d_{5/2}^{-1}5d$ and $4d_{3/2}^{-1}5d'$ were observed by King *et al.*,[9] but their intensities are very weak. To the best of our knowledge, it is the only work to study the optically forbidden transitions of the 4d electron of xenon.

In this paper, the dipole-forbidden excitations of the 4d electron of xenon are studied by the electron impact method with a large momentum transfer, and new information of $4d^{-1}ns$ and $4d^{-1}nd$ is reported.

2. Experimental and theoretical methods

In this work, the angle-resolved electron energy loss spectrometer, which has been described in detail in our previous works,[29,30] was used. In the present experiment, the spectrometer was operated at an incident electron energy of 1.5 keV and a scattering angle of 6°, which corresponds to a squared momentum transfer of 1.20 a.u. (atomic unit). The electron energy loss spectra in the energy regions of 7 eV–9 eV and 62 eV–70 eV were recorded simultaneously at a sample pressure of 8.2×10^{-3} Pa. The energy resolution and the instrumental function of the spectrometer were determined from the observed peak of $5p^5 6s[3/2]_1$ in 7 eV–9 eV because of its negligible natural width, and the former is 90 meV. The instrumental function of the spectrometer is used to deconvolve the peak profiles of the inner-shell excitations of the 4d electron in 62 eV–70 eV which will be described below. The measured spectrum is shown in Fig. 1, and the features are assigned according to our calculation (see Table 1) and the previous investigations.[9]

The measured spectrum shown in Fig. 1 is the one of the real spectrum convoluted by the instrumental function, and the least-squares fitting was used to determine the line profile parameters such as the energy positions and natural widths of the inner-shell transitions. The fitting function for a peak is expressed as follows:

$$F(x) = \int V(t,a_1,a_2,a_3,a_4)\cdot L(x-t,b_1,b_2,b_3)\mathrm{d}t, \qquad (1)$$

where

$$V(t,a_1,a_2,a_3,a_4) = \frac{a_1 a_4}{\pi^{3/2}a_3}\int \frac{\exp(-s^2)}{a_4^2+\left(\frac{t-a_2}{a_3}-s\right)^2}\mathrm{d}s, \qquad (2)$$

$$L(x-t,b_1,b_2,b_3) = \frac{b_1}{\pi b_3\left[1+\left(\frac{x-t-b_2}{b_3}\right)^2\right]}. \qquad (3)$$

Here the Voigt function $V(t,a_1,a_2,a_3,a_4)$ is used to describe the instrumental function, and $L(x-t,b_1,b_2,b_3)$ is the Lorentz function. a_1, a_2, a_3, a_4, b_1, b_2, and b_3 are all fitting parameters. As mentioned above, the instrumental function $V(t,a_1,a_2,a_3,a_4)$ was determined by fitting the peak of $5p^5 6s[3/2]_1$. It is believed that the Lorentz function can represent the true line profiles of inner-shell excitations of xenon, since the peak is almost symmetric as shown in Fig. 1 which means that the interaction between the discrete excitation and the ionization continuum is negligible. The same assumption has been used in all previous investigations.[19–21] Then a function obtained by convolving the instrumental function with a Lorentz function whose central position and line width are variable is used to fit the inner-shell excitations, and the fitted results are also shown in Fig. 1.

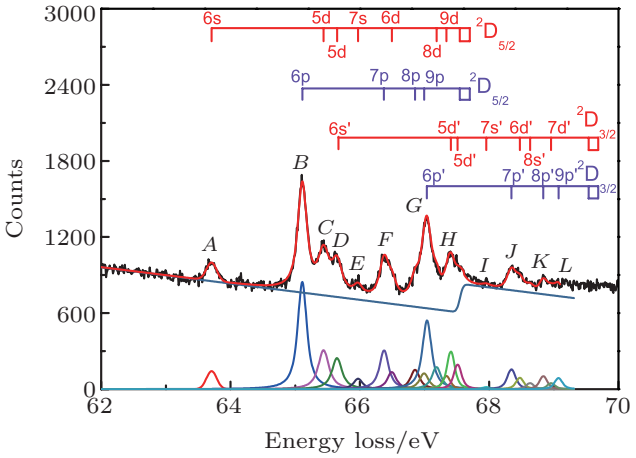


Fig. 1. (color online) The electron energy loss spectrum of xenon measured at an impact energy of 1500 eV and a scattering angle of 6°. Herein the prime in the electronic configuration means the Rydberg series converges to $4d^9 {}^2D_{3/2}$, in order to distinguish with the Rydberg series converging to $4d^9 {}^2D_{5/2}$.

In order to assign the measured features shown in Fig. 1, especially for the dipole-forbidden ones, the Cowan code[31] was used to calculate the excitation energies and the intermediate coupling coefficients of the 4d excitations. The method of the calculation was described in detail by Clark *et al.*[32,33] and summarized briefly in our recent work.[27,34] For the present calculations a 26-configuration basis set was used, and the calculated excitation energies as well as the intermediate coupling coefficients are listed in Table 1. In the calculation, the interaction between the discrete state and the ionization continuum was ignored. In addition, the *JL* designation was adopted.

Table 1. The energies, intermediate-coupling coefficients and the assignments for the peaks from *A* to *L* as shown in Fig. 1. Some weak transitions are not included for clarity. The energy levels from our calculations and this experiment are given. E_0, E_1, E_2, and E_3 represent the electric monopole, electric dipole, electric quadrupole, and electric octupole transitions from the ground state, respectively. The terms whose intermediate-coupling coefficients are less than 0.2 are neglected.

Peak	*JL* designation	Intermediate coupling	Transition	Energy/eV[a] Cowan	Energy/eV Experiment
	$4d^{10}5s^25p^6\ ^1S_0$	$1.0(5p^6\,^1S_0)$			0
A	$4d^96s[5/2]_2$	$0.64(4d^96s^1D_2)+0.77(4d^96s^3D_2)$	E_2	63.75	63.707
B	$4d^96p[7/2]_3$	$0.69(4d^96p^1F_3)+0.73(4d^96p^3F_3)$	E_3	65.052	65.110[b]
	$4d^96p[3/2]_1$	$-0.31(4d^96p^1P_1)-0.33(4d^96p^3P_1)+0.89(4d^96p^3D_1)$	E_1	65.086	
	$4d^96p[5/2]_3$	$-0.30(4d^96p^1F_3)+0.92(4d^96p^3D_3)+0.26(4d^96p^3F_3)$	E_3	65.109	
C	$4d^95d[5/2]_2$	$-0.42(4d^95d^1D_2)+0.90(4d^95d^3F_2)$	E_2	65.443	65.439
	$4d^95d[3/2]_2$	$-0.57(4d^95d^3P_2)+0.42(4d^95d^1D_2)$ $+0.29(4d^95d^3F_2)+0.64(4d^95d^3D_2)$	E_2	65.485	
D	$4d^95d[1/2]_0$	$-0.68(4d^95d^1S_0)+0.63(4d^95d^3P_0)$	E_0	65.593	65.647
	$4d^96s'[3/2]_2$	$0.77(4d^96s^1D_2)-0.64\ (4d^96s^3D_2)$	E_2	65.623	
E	$4d^97s[5/2]_2$	$0.63(4d^97s^1D_2)+0.77(4d^97s^3D_2)$	E_2	65.974	65.972
	$4d^97p[3/2]_1$	$-0.31(4d^97p^1P_1)-0.35(4d^97p^3P_1)+0.88(4d^97p^3D_1)$	E_1	66.358	66.375[b]
F	$4d^96d[5/2]_2$	$-0.42(4d^96d^1D_2)+0.89\ (4d^96d^3F_2)$	E_2	66.435	66.495
	$4d^96d[3/2]_2$	$0.59(4d^96d^3P_2)+0.40(4d^96d^1D_2)$ $+0.64(4d^96d^3D_2)+0.29(4d^96d^3F_2)$	E_2	66.453	
	$4d^96d[1/2]_0$	$-0.65(4d^96d^1S_0)+0.73\ (4d^95d^3P_0)$	E_0	66.505	
G	$4d^96p'[3/2]_1$	$0.55(4d^96p^1P_1)+0.70(4d^96p^3P_1)+0.45(4d^96p^3D_1)$	E_1	67.041	67.039[b]
	$4d^96p'[1/2]_1$	$0.77(4d^96p^1P_1)-0.63(4d^96p^3P_1)$	E_1	67.085	
H	$4d^95d'[5/2]_2$	$0.80(4d^95d^3P_2)+0.25(4d^95d^1D_2)+0.54(4d^95d^3D_2)$	E_2	67.458	67.408
	$4d^95d'[3/2]_2$	$0.76(4d^95d^1D_2)-0.54(4d^95d^3D_2)+0.33(4d^95d^3F_2)$	E_2	67.479	
	$4d^95d'[1/2]_0$	$0.72(4d^95d^1S_0)+0.65(4d^95d^3P_0)$	E_0	67.598	67.513
I	$4d^97p'[3/2]_1$	$0.55(4d^97p^1P_1)+0.69(4d^97p^3P_1)+0.47(4d^97p^3D_1)$	E_1	68.335	68.345[b]
	$4d^97p'[1/2]_1$	$0.77(4d^97p^1P_1)-0.63(4d^97p^3P_1)$	E_1	68.35	
	$4d^96d'[5/2]_2$	$0.79(4d^96d^3P_2)+0.28(4d^96d^1D_2)+0.54(4d^96d^3D_2)$	E_2	68.434	68.475
	$4d^96d'[3/2]_2$	$0.77(4d^96d^1D_2)-0.54(4d^96d^3D_2)+0.34(4d^96d^3F_2)$	E_2	68.443	
	$4d^96d'[1/2]_0$	$0.74(4d^96d^1S_0)+0.66(4d^96d^3P_0)$	E_0	68.488	

[a]The calculated energies were shifted by 0.1 eV to match the measured spectra better.

[b]The energy levels are taken from Ref. [9]

3. Results and discussions

From Fig. 1, it can be seen that at the scattering angle of 6°, not only the optically allowed transitions of $4d_{5/2}^{-1}np$ and $4d_{3/2}^{-1}np'$, but also the optically forbidden transitions of $4d_{5/2}^{-1}ns$, $4d_{5/2}^{-1}nd$, $4d_{3/2}^{-1}ns'$, and $4d_{3/2}^{-1}nd'$, were observed. The energy level positions and natural widths of some transitions were determined by the least-squares fitting, and the results are listed in Tables 1 and 2.

Firstly, we concentrate on the dipole-allowed transitions of $4d_{5/2}^{-1}np$ and $4d_{3/2}^{-1}np'$ since they were studied extensively. It is clear from Table 1 that the peak *B* includes both of the dipole-allowed transition of $4d_{5/2}^{-1}6p[3/2]_1$ and the dipole-forbidden ones of $4d_{5/2}^{-1}6p[7/2]_3$, and $4d_{5/2}^{-1}6p[5/2]_3$, since the intervals of about 30 meV among them are less than the present experimental energy resolution of 90 meV. Actually, in the initial trial fitting procedure, the octupole-allowed transitions of $4d_{5/2}^{-1}6p[7/2]_3$ and $4d_{5/2}^{-1}6p[5/2]_3$ were included, but it gives negligible intensities. So in the final data fitting, these two dipole-forbidden transitions were ignored. Considering that the higher states of $4d_{5/2}^{-1}np[7/2]_3$ and $4d_{5/2}^{-1}np[5/2]_3$ ($n \geq 7$) should have much lower intensities than those of $4d_{5/2}^{-1}6p[7/2]_3$ and $4d_{5/2}^{-1}6p[5/2]_3$, their contributions to the $4d_{5/2}^{-1}np[3/2]_1$ are ignored too, and the calculated results for them are not shown in Table 1 for clarity. Similarly, the dipole-forbidden transitions of $4d_{3/2}^{-1}np'[5/2]_3$ which are near to $4d_{3/2}^{-1}np'[3/2]_1$ and $4d_{3/2}^{-1}np'[1/2]_1$, are ignored. Therefore, for the dipole-allowed transitions, we only consider the $4d_{5/2}^{-1}np[3/2]_1$, $4d_{3/2}^{-1}np'[3/2]_1$, and $4d_{3/2}^{-1}np'[1/2]_1$, while the contributions from the nearby transitions of the octupole-allowed ones are neglected with the reasons mentioned above.

Since the accurate energy level positions of the dipole-allowed transitions have been determined by the previous EELS works[9] and synchrotron radiation ones,[18] as well as

the energy resolution of 90 meV in this work is slightly worse than the previous ones, in the least-squares fitting procedure the energy positions of the dipole-allowed excitations were fixed on the ones reported by King *et al.*[9] Considering the heavy overlapping of the transitions above 64 eV, fixing the energy positions of the dipole-allowed transitions can reduce the fitting errors of the natural widths of these transitions and the parameters of other dipole-forbidden ones.

It can be seen from Table 2 that the best agreement of the natural widths measured by different groups is achieved for the $4d_{5/2}^{-1}6p[3/2]_1$, which is well separated from other transitions in the measured spectrum under the optical condition. The only exception is that the result of Masui *et al.*[21] is slightly lower than others and the deviation is beyond the experimental errors. As for the natural widths of other dipole-allowed transitions of $4d_{5/2}^{-1}np$ and $4d_{3/2}^{-1}np'$, the early results of King *et al.*[9] and Ederer *et al.*[18] are more scattered, i.e., some values are too high and some values are too low. The recent results of Refs. [19] and [21] and ours are in better agreement although the present results are slightly higher and the ones of Masui *et al.*[21] are slightly lower. It is difficult to give a definite answer to which one is more reliable. The present energy resolution is worse than those of Sairanen *et al.*[19] and Masui *et al.*,[21] and the observed dipole-forbidden transitions in this work aggravate the situation. However, we can accurately determine the instrumental function from the peak profile of $5p^5 6s[3/2]_1$, which is crucial to obtain the accurate natural widths. Although the synchrotron radiation experiments[19,21] have the high energy resolutions, it is difficult to accurately determine the instrumental function since it depends on the photon energy. Refs. [9], [19], and [21] surmised that the instrumental function is Gaussian while the inner-shell transitions have the peak profiles of Lorentz. It should be mentioned that according to our calculation shown in Table 1, the dipole-allowed transition of $4d_{3/2}^{-1}6p'$ should include two transitions, i.e., $4d^9 6p'[3/2]_1$ and $4d^9 6p'[1/2]_1$, and their interval is about 40 meV. So considering that the natural widths for the inner-shell excitations are nearly independent of the principal quantum number n (Ref. [35]) and have almost equal values, the width of $4d_{3/2}^{-1}6p'$ that has fine structure ($4d^9 6p'[3/2]_1$ and $4d^9 6p'[1/2]_1$) should be larger than that of the single transition $4d_{5/2}^{-1}6p[3/2]_1$. The present experiment follows this theoretical prediction, i.e., the width of 119 meV for $4d_{3/2}^{-1}6p'$ is slightly larger than the one of 113 meV for $4d_{5/2}^{-1}6p[3/2]_1$. However, both recent results based on the synchrotron radiation[19,21] are reversed. Similar to $4d_{3/2}^{-1}6p'$, the transition of $4d_{3/2}^{-1}7p'$ also includes two transitions ($4d^9 7p'[3/2]_1$ and $4d^9 7p'[1/2]_1$), and their natural widths are nearly independent of the principal quantum number n. However, the energy interval of these two transitions is only about 15 meV, which is much less than their natural widths. Considering the uncertainties of the obtained natural widths, it is reasonable that the width of 112 meV for $4d_{3/2}^{-1}7p'$ is close to the one of 113 meV for $4d_{5/2}^{-1}7p[3/2]_1$.

Besides the dipole-allowed transitions mentioned above, abundant dipole-forbidden ones, which are absent in the previous experimental studies, are also observed in the measured spectrum as shown in Fig. 1. The energy position and natural width of the quadrupole transition of $4d_{5/2}^{-1}6s[5/2]_2$ determined by this work are reliable because of its individual character. It is clear from Table 2 that the natural width of $4d_{5/2}^{-1}6s[5/2]_2$ is approximately identical with those of the dipole-allowed ones. A similar phenomenon was observed in the 3d excitations of krypton.[36] These phenomena may be due to the fact that the resonant Auger effect is dominated by the spectator transitions in the 4d excitations of xenon and 3d excitations of krypton. So the total decay rate is little affected by the excited spectator electron in the different orbitals which was pointed out in Ref. [35].

Table 2. Natural widths of Xe-4d excitations (the numbers in parentheses are standard errors with the units of meV).

State		Energy level/eV	Present	Ref. [9]	Natural width/meV Ref. [18]	Ref. [19]	Ref. [21]
$4d_{5/2}^{-1}$	6s	63.707(5)	102(10)				
	6p	65.110(10)[a]	113(2)	111(4)	114(8)	109.8(1)	106.3(0.5)
	5d	65.439(4)					
	5d + 6s′	65.647(5)					
	7s	65.972(11)					
	7p	66.375(2)[a]	113(14)	128(9)	90(2)	109(1)	106.0(0.5)
	6d	66.495(8)					
	edge	67.548(1)[a]					
$4d_{3/2}^{-1}$	6p′	67.039(2)[a]	119(6)	119(8)	130(3)	107(1)	104(1)
	5d′	67.408(27)					
	5d′	67.513(24)					
	7p′	68.345(3)[a]	112(8)	133(15)	110(3)	106(3)	106(5)
	6d′	68.475(14)					
	edge	69.537(2)[a]					

[a]The energy levels are taken from Ref. [9]

The quadrupole transition of $4d_{5/2}^{-1}7s[5/2]_2$ is too weak to draw the information of its natural width and only its energy position is reported and listed in Table 2. The dipole-forbidden features of *C* and *D* shown in Fig. 1 consist of four transitions, that is, the quadrupole-allowed transitions of $4d_{5/2}^{-1}5d[5/2]_2$, $4d_{5/2}^{-1}5d[3/2]_2$, $4d_{3/2}^{-1}6s'[3/2]_2$, and monopole-allowed transition of $4d_{5/2}^{-1}5d[1/2]_0$, while the measured spectrum by King *et al.*[9] shows only one feature due to their small momentum transfer and poor statistics. Based on our calculation shown in Table 1, they are separated into two groups according to their intervals, and each of them has an interval of about 40 meV. Considering that the present energy resolution is only about 90 meV and the natural widths of them are all about 110 meV, we can only give the peak positions of features *C* and *D*, i.e., 65.439 eV and 65.647 eV, as shown in Table 2. Similarly, the energy positions of $4d_{5/2}^{-1}6d$, $4d_{3/2}^{-1}5d'$, and $4d_{3/2}^{-1}6d'$ are reported. The present results of the positions of $4d_{5/2}^{-1}5d$ and $4d_{3/2}^{-1}5d'$ are close to the results of 65.446 eV and 67.411 eV of King *et al.*,[9] and the present ones are more reliable due to the good statistics and the larger momentum transfer.

4. Summary and conclusion

The electron energy loss spectrum of 4d excitations of xenon has been measured at an incident electron energy of 1500 eV and a scattering angle of 6°. Not only the optically allowed transitions of $4d_{5/2}^{-1}np$ and $4d_{3/2}^{-1}np'$ but also the optically forbidden transitions of $4d_{5/2}^{-1}ns$, $4d_{5/2}^{-1}nd$, $4d_{3/2}^{-1}ns'$, and $4d_{3/2}^{-1}nd'$ have been observed. By fitting the measured spectrum, the line profile parameters of these excitations were determined. It is found that the present natural widths of both the quadrupole-allowed transition of $4d_{5/2}^{-1}6s[5/2]_2$ and the dipole-allowed ones are nearly identical and independent of the main quantum number *n* within the experimental errors. In addition, the present natural widths are in general agreement with the recent synchrotron radiation ones.[19,21] The above phenomena may be due to that the spectator transitions dominate the resonant Auger effect for both dipole-allowed and dipole-forbidden transition. Furthermore, many dipole-forbidden transitions were observed, and the energy positions of these features are reported. However, in order to obtain the detailed information, more high-resolution experiments and elaborate theoretical calculations are strongly recommended.

References

[1] Fano U 1961 *Phys. Rev.* **124** 1866
[2] Tanner G, Richter K and Rost J M 2000 *Rev. Mod. Phys.* **72** 497
[3] Eberhardt W, Kalkoffen G and Kunz C 1978 *Phys. Rev. Lett.* **41** 156
[4] Ricz S, Kövér Á, Jurvansuu M, Varga D, Molnar J and Aksela S 2002 *Phys. Rev. A* **65** 042707
[5] Huttula S -M, Heinäsmäki S, Aksela H, Tulkki J, Kivimäki A, Jurvansuu M and Aksela S 2001 *Phys. Rev. A* **63** 032703
[6] Domke M, Mandel T, Puschmann A, Xue C, Shirley D A, Kaindl G, Petersen H and Kuske P 1992 *Rev. Sci. Instrum.* **63** 80
[7] Zangrando M, Zacchigna M, Finazzi M, Cocco D, Rochow R and Parmigiani F 2004 *Rev. Sci. Instrum.* **75** 31
[8] Quaresima C, Ottaviani C, Matteucci M, Crotti C, Antonini A, Capozi M, Rinaldi S, Luce M, Perfetti P, Prince K C, Astaldi C, Zacchigna M, Romanzin L and Savoia A 1995 *Nucl. Instrum. Methods Phys. Res. A* **364** 374
[9] King G C, Tronc M, Read F H and Bradford R C 1977 *J. Phys. B: At. Mol. Phys.* **10** 2479
[10] Hitchcock A P and Brion C E 1978 *J. Electron Spectrosc. Relat. Phenom.* **14** 417
[11] Shaw D A, King G C, Read F H and Cvejanović D 1982 *J. Phys. B: At. Mol. Phys.* **15** 1785
[12] Codling K and Madden R P 1972 *J. Res. Natl. Bur. Stand., Sec. A* **76** 1
[13] Codling K and Madden R P 1964 *Phys. Rev. Lett.* **12** 106
[14] Codling K and Madden R P 1971 *Phys. Rev. A* **4** 2261
[15] Madden R P, Ederer D L and Codling K 1969 *Phys. Rev.* **177** 136
[16] Codling K, Madden R P and Ederer D L 1967 *Phys. Rev. A* **155** 26
[17] Nakamura M, Sasanuma M, Sato S, Watanabe M, Yamashita H, Iguchi Y, Ejiri A, Nakai S, Yamaguchi S, Sagawa T, Nakai Y and Oshio T 1968 *Phys. Rev. Lett.* **21** 1303
[18] Ederer D L and Manalis M 1975 *J. Opt. Soc. Am.* **65** 634
[19] Sairanen O P, Kivimäki A, Nõmmiste E, Aksela H and Aksela S 1996 *Phys. Rev. A* **54** 2834
[20] Jurvansuu M, Kivimäki A and Aksela S 2001 *Phys. Rev. A* **64** 012502
[21] Masui S, Shigemasa E, Yagishita A and Sellin I A 1995 *J. Phys. B: At. Mol. Opt. Phys.* **28** 4529
[22] Prince K C, Vondráček M, Karvonen J, Coreno M, Camilloni R, Avaldi L and de Simone M 1999 *J. Electron Spectrosc. Relat. Phenom.* **101** 141
[23] Zhu L F, Cheng H D, Liu X J, Tian P, Yuan Z S, Li W B and Xu K Z 2003 *Chin. Phys. Lett.* **20** 1718
[24] Yuan Z S, Sakai Y, Umeda N, Fujita Y, Takayanagi T, Yamada C, Nakamura N, Ohtani S, Zhu L F and Xu K Z 2006 *J. Phys. B: At. Mol. Opt. Phys.* **39** 5097
[25] Jiang W C, Zhu L F and Xu K Z 2008 *Chin. Phys. Lett.* **25** 3649
[26] Ge M, Zhu L F, Liu C D and Xu K Z 2008 *Chin. Phys. Lett.* **25** 3646
[27] Ren L M, Wang Y Y, Li D D, Yuan Z S and Zhu L F 2011 *Chin. Phys. Lett.* **28** 053401
[28] Boechat-Roberty H M, Freitas J D, Almeida D P and de Souza G G B 2002 *J. Phys. B: At. Mol. Opt. Phys.* **35** 1409
[29] Wu S L, Zhong Z P, Feng R F, Xing S L, Yang B X and Xu K Z 1995 *Phys. Rev. A* **51** 4494
[30] Liu X J, Zhu L F, Jiang X M, Yuan Z S, Cai B, Chen X J and Xu K Z 2001 *Rev. Sci. Instrum.* **72** 3357
[31] Cowan R D 1981 *The Theory of Atomic Structure and Spectra* (Berkeley: University of California Press)
[32] Clark R E H, Abdallah J, Csanak G and Kramer S P 1989 *Phys. Rev. A* **40** 2935
[33] Clark R E H, Csanak G and Abdallah J 1991 *Phys. Rev. A* **44** 2874
[34] Cheng H D, Zhu L F, Yuan Z S, Liu X J, Sun J M, Jiang W C and Xu K Z 2005 *Phys. Rev. A* **72** 012715
[35] Armen G B, Aksela H, Åberg T and Aksela S 2000 *J. Phys. B: At. Mol. Opt. Phys.* **33** R49
[36] Yuan Z S, Zhu L F, Liu X J, Li W B, Cheng H D, Sun J M and Xu K Z 2005 *Phys. Rev. A* **71** 064701